Supporting information

Amorphous-crystalline Heterostructured Niobium Oxide as Two-in-One Host Matrix for High-Performance Lithium-Sulfur Batteries

Jiayi Wang[a†], Gaoran Li[d†], Dan Luo[a], Yan Zhao[b]*, Yongguang Zhang[a,b]*, Guofu Zhou[c], Lingling Shui[a], Xin Wang[a,c]*

Experimental section

Synthesis of PMMA: Repeated wash by 0.1 M NaOH solution and deionized water was employed to remove the inhibitor in methyl methacrylate (MMA). Following reduced-pressure distillation was used to purify the MMA. 140 mL deionized water was added into the flask and was heated to 70 °C. After removing the air by Ar inlet, 40 mL MMA was added into the heated water as well as the solution containing 0.15 g V50 and 10 mL deionized water. Constant stir for 4 h was conducted under the Ar at 70 °C to produce PMMA. Afterwards, the synthesized PMMA was collected by suction filtration using filtration membrane. The obtained PMMA solution was put in a ventilated place and dried naturally.

Synthesis of Nb_2O_5: 0.01 mol $NbCl_5$ was dissolved into 20 mL ethanol to prepare the precursor solution. Prepared PMMA array was immersed into the precursor solution for 24 h. Following dry at 60 °C was used to remove the extra ethanol. A-Nb_2O_5/A/T-Nb_2O_5/T-Nb_2O_5 was synthesized by following calcination for 2 h at 400/550/700 °C with a heating rate of 1 °C min^{-1} under the air atmosphere.

Synthesis of S-Nb_2O_5: The synthesized Nb_2O_5 was mixed with sulfur with a mass ratio of 1:4. Following calcination at 155 °C for 12 h was conducted to disperse the sulfur uniformly under Ar. Extra calcination at 200 °C for 1 h was employed to remove the sulfur on the surface of Nb_2O_5.

Sulfur Cathode Test: In order to analyze the electrochemical performance of synthesized Nb_2O_5, the battery was assembled in a glove box filled with Ar. The cathode material was formed by mixing Nb_2O_5, super P and PVDF according to a mass ratio of 8:1:1. The mixture was dissolved in the N-Methyl pyrrolidone (NMP) to obtain

a slurry, which was casted on the carbon coated Al foil to prepare the working electrode. The prepared electrode was cut into disc with a diameter of 9 mm to serve as cathode. Lithium foil was used as the anode and the electrolyte was 1 M bis (trifluoromethane) sulfonimide lithium (LiTFSI) in 1, 2-dimethoxyethane (DME) and 1, 3-dioxopentane (DOL) (volume ratio is 1:1) with 1 wt.% $LiNO_3$ additive. The Neware battery test system (BTS-5V5 mA) was used to explore the electrochemical performance. Cyclic voltammetry (CV) and electrochemical impedance spectroscopy were carried out on the electrochemical workstation (Bio-logic VSP-300). The CV curve was tested at the scanning rate of 0.1 mV s^{-1} under the charge-discharge voltage range of 1.7 ~ 2.8 V. The frequency range measured in EIS test is 100 kHz~0.01 mHz. The regular sulfur loading of the prepared electrode was ~1.5 mg cm^{-2} and the electrolyte amount was 30 μL.

Assembly of Li_2S_6 Symmetric Cells: Symmetrical batteries were assembled in a glove box filled with Ar. Li_2S_6 electrolyte was prepared by mixing Li_2S with sulfur powder at the molar ratio of 1:5 and stirring at 60 °C for 24 h in an Ar-filled glove box. The electrode of symmetrical battery was prepared by dispersing Nb_2O_5 on carbon cloth. Measurement of CV and EIS of symmetrical battery was conducted on the electrochemical workstation (Bio-logic VSP-300).

LSV Measurement: Ag/AgCl was used as reference electrodes, and 0.1 M Li_2S/methanol was used as electrolyte. The prepared Nb_2O_5, PVDF and super P were mixed in a mass ratio of 8:1:1 and dropped on the surface of glassy carbon electrode with NMP as solvent. Electrochemical workstation (Bio-logic VSP-300) was used to measure the LSV curves.

Li_2S Nucleation Test: The synthesized composite was dispersed on carbon cloth with ethyl alcohol as solvent to prepare working electrode. 0.5 M Li_2S_8/tetraethylene glycol dimethyl ether solution was used as electrolyte and the lithium foil was employed as anode. The assembled battery was discharged at 0.112 mA with a constant current until the voltage drops to 2.06 V, and then discharged at 2.05 V until the current drops below 10^{-5} A.

Li_2S_6 Adsorption Test: Li_2S_6 solution was prepared by constantly stirring at 60 °C

for 24 h in an argon-filled glove box with a molar ratio of Li_2S to sulfur powder of 1: 5 in above mentioned electrolyte. The synthesized composite was added into Li_2S_6 solution (5 mM) and adsorbed for 6 hours, and the color change of Li_2S_6 solution was observed. After adsorption, the separated supernatant was tested by UV-vis spectrum.

Lithium Metal Anode Test: The working electrodes were prepared by casting A/T-Nb_2O_5 and PVDF (mass ratio is 9:1) on the Cu foil using NMP as solvent. The battery was fabricated using lithium foil as anode and the above-mentioned electrolyte. The initial five cycles from 0~1 V with a current of 0.05 mA was conducted to produce a stable solid-electrolyte interface. In the cycle test, 0.5 mAh cm^{-2} of Li was first plated and then stripped on the working electrode with a current density of 0.5 mA cm^{-2} for 1 h, respectively, from −1~1 V. In the symmetrical cell test, 3 mAh cm^{-2} of Li was first plated on the working electrode with a current density of 0.5 mA cm^{-2}, then the cycle test was conducted at 0.5 mA cm^{-2} for 1 h in the corresponding plant and strip cycle.

Full Li-S Cell Tests: Full Li-S cells were fabricated with Li-A/T-Nb_2O_5 as the anode and S-A/T-Nb_2O_5 as the cathode. 10 mAh cm^{-2} of Li metal was pre-planted on the working electrode to prepare Li-A/T-Nb_2O_5 anode. S-A/T-Nb_2O_5 cathode and the electrolyte are same with the sulfur cathode test. The used equipment is same with the sulfur cathode test.

Theoretical Calculations: In our work, the Nb_2O_5 structure was optimized based on first-principles and it was found that it has the following lattice parameters: a =3.41 Å, b = 4.54 Å, c = 11.74 Å. It is known that the amorphous structure can be obtained using ab initio molecular dynamics (AIMD) methods. In other words, the crystal structure will be transformed into an amorphous structure by simulating a liquid phase of the desired composition and quench it in order to find a non-crystalline local minimum. Therefore, the 2×2×1 supercell has been simulated annealing to produce the amorphous Nb_2O_5 with 10 ps at canonical ensemble (NVT) using AIMD, compatibly with computational limitations. The other density functional theory (DFT) calculation was based on plane-wave ultra-soft pseudopotential method and Perdew-Burke-Ernzerhof (PBE) for the exchange and correlation energy terms. The cut off energy of plane wave was 400 eV, and the Monkhorst-Pack grid k-space was set to be 2×2×1.

The maximal interaction forces of atoms were 0.03 eV Å^{-1}.

Material Characterizations: The crystal structure was analyzed by XRD (D8 Focus, Bruker). The morphology was observed by scanning electron microscope (SEM, ZEISS Gemini 500) and transmission electron microscope (TEM, JEM-2100HR, JEOL). Raman spectra were photographed with Raman microscope (Thermo Scientific, Waltham, MA). The specific surface area and pore distribution of the materials were calculated by Brunnauer-Emmett-Teller (BET) based on Barret-Joyner-Halenda (BJH) method using V-Sorb 2800P. The chemical configuration was explored by X-ray photoelectron spectroscopy (XPS, PHI5000). Thermogravimetric analysis (TGA) was carried out with a thermogravimetric analyzer (TA-DTG Q600) under N_2 with a heating rate of 10 °C min^{-1}.
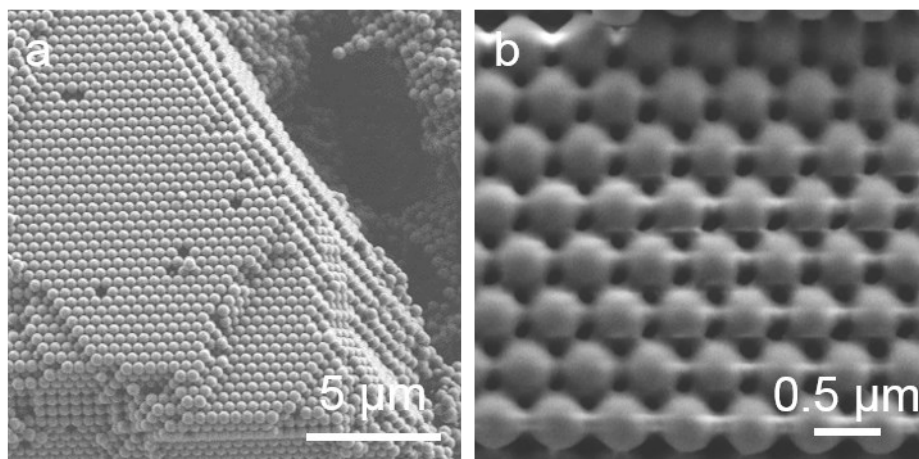
Figure S1. (a, b) SEM images of prepared PMMA spheres.
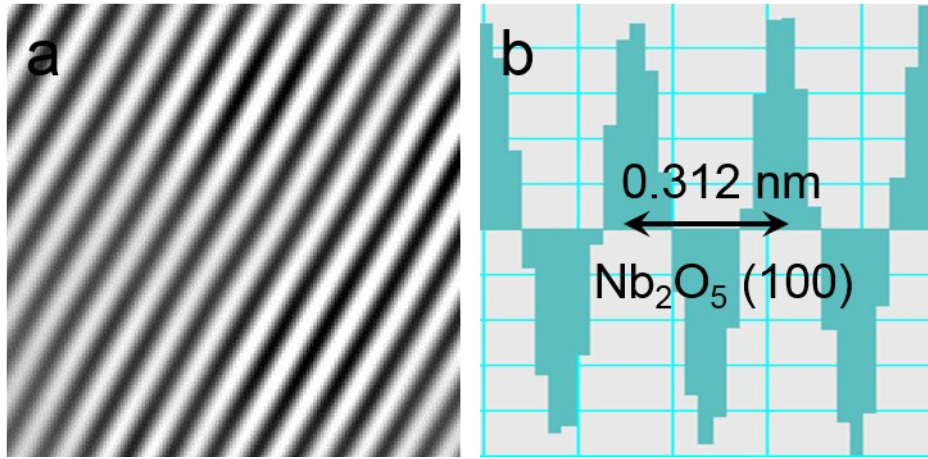
Figure S2. (a) inverse FFT pattern and (b) lattice spacing of the green selected area of Figure 2e.
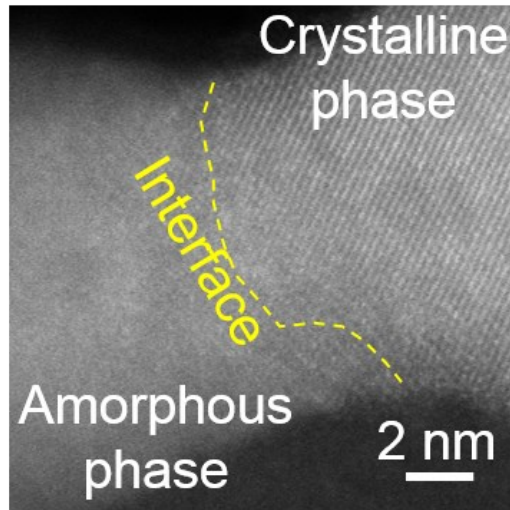
Figure S3. STEM image of A/T-Nb_2O_5.
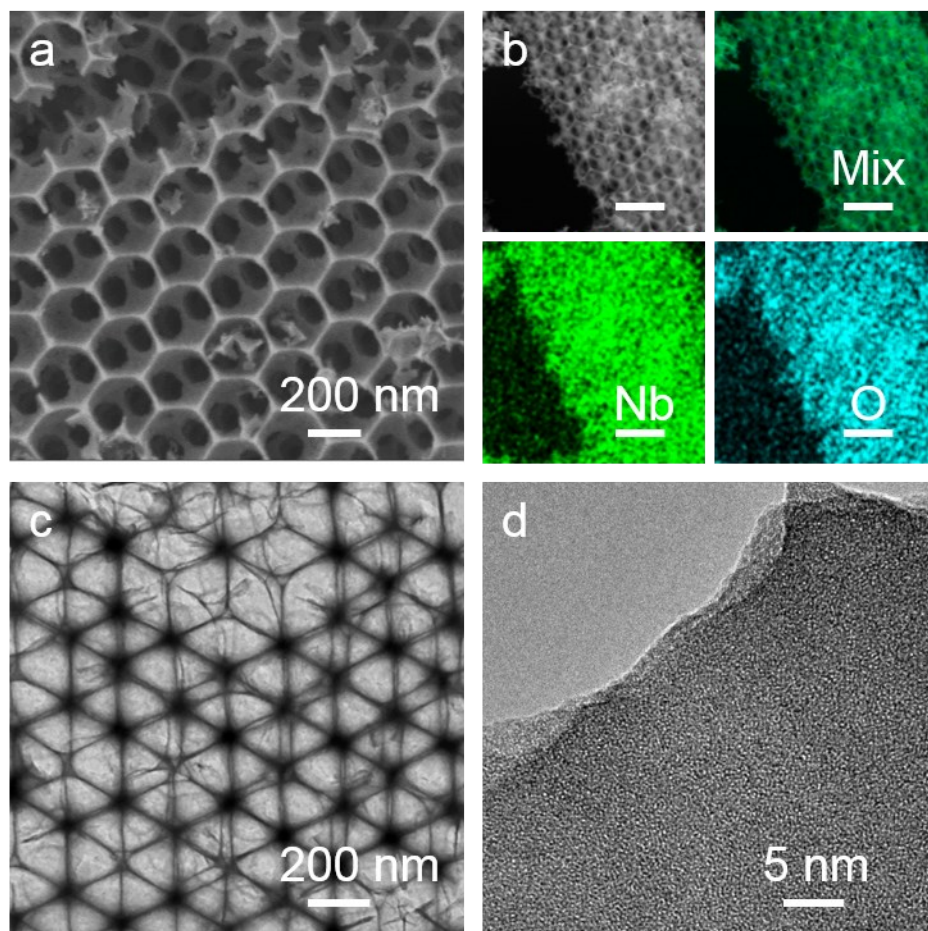
Figure S4. (a) SEM image, (b) the element distribution mapping with a scale bar of 500 nm, (c) TEM image and (d) HRTEM image of A-Nb_2O_5.
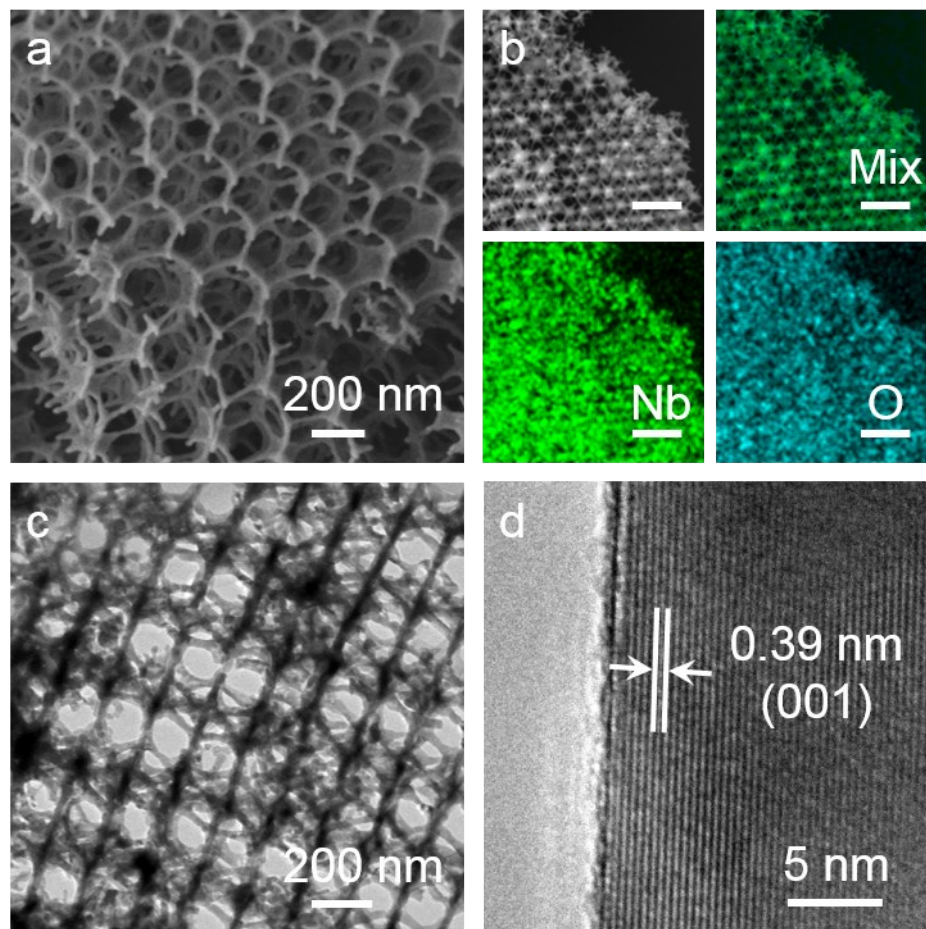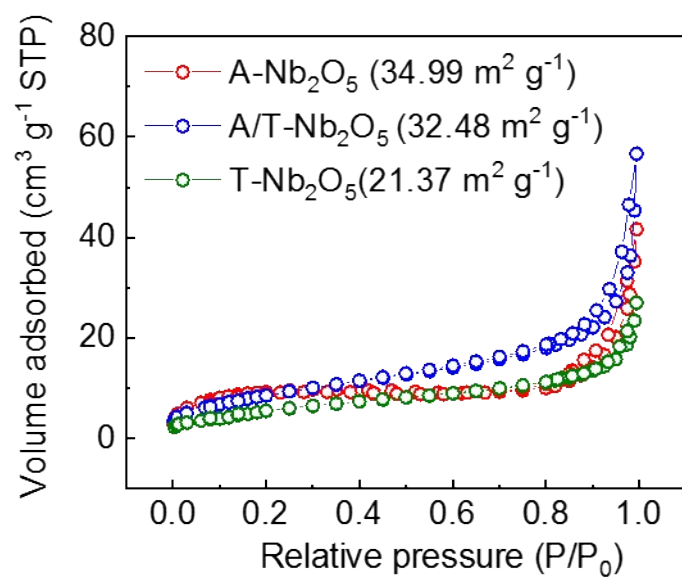
Figure S5. (a) SEM image, (b) the element distribution mapping with a scale bar of 500 nm, (c) TEM image and (d) HRTEM image of T-Nb$_2$O$_5$.

Figure S6. N_2 adsorption/desorption isotherms of A-Nb_2O_5, A/T-Nb_2O_5 and T-Nb_2O_5.
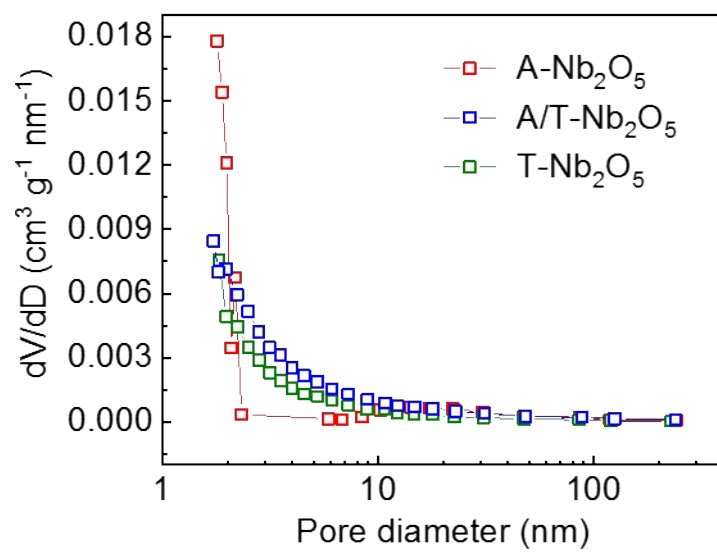
Figure S7. Pore distribution of A-Nb$_2$O$_5$, A/T-Nb$_2$O$_5$ and T-Nb$_2$O$_5$.
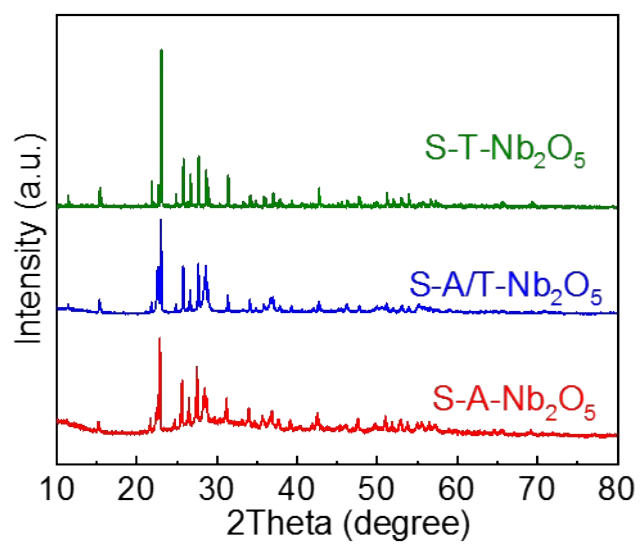
Figure S8. XRD patterns of S-A-Nb$_2$O$_5$, S-A/T-Nb$_2$O$_5$ and S-T-Nb$_2$O$_5$.
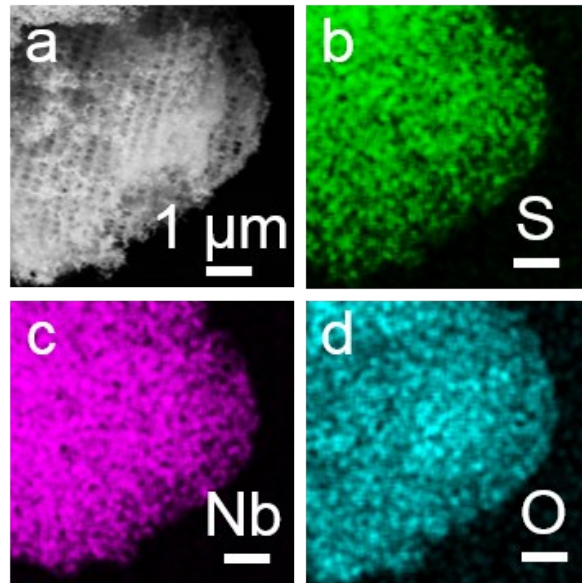
Figure S9. SEM image of S-A/T-Nb$_2$O$_5$ and the corresponding element mapping.
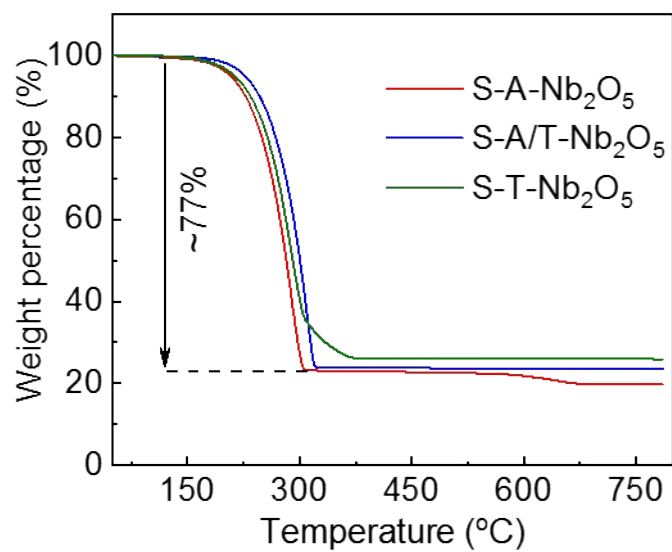
Figure S10. TGA curves of S-A-Nb_2O_5, S-A/T-Nb_2O_5 and S-T-Nb_2O_5 hybrids.
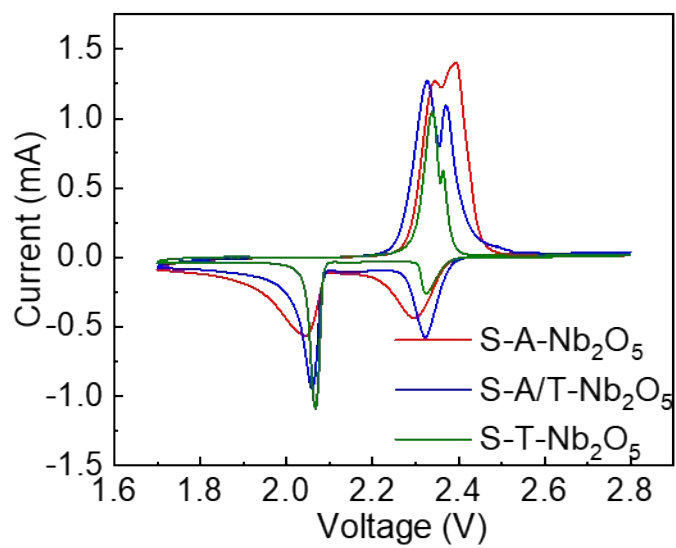
Figure S11. CV curves of the cells with S-A-Nb$_2$O$_5$, S-A/T-Nb$_2$O$_5$ and S-T-Nb$_2$O$_5$ electrodes.
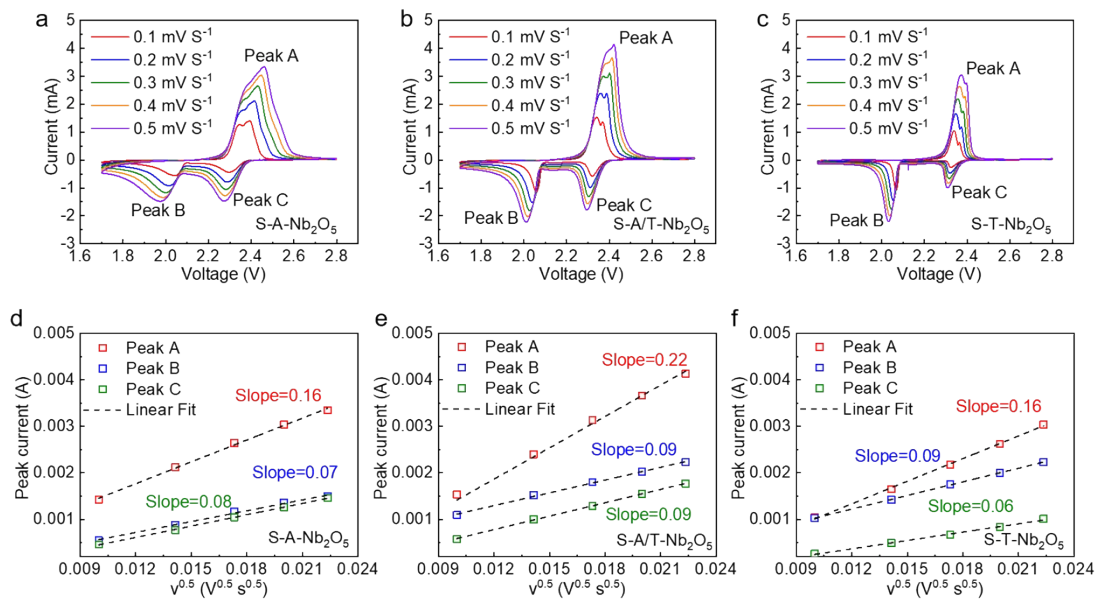
Figure S12. (a–c) CV curves at different scan rates, and (d–f) the corresponding linear fitting based on Randles–Sevick equation.

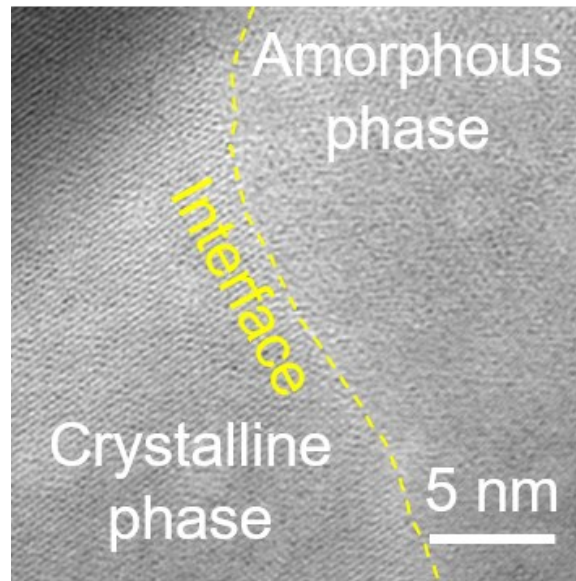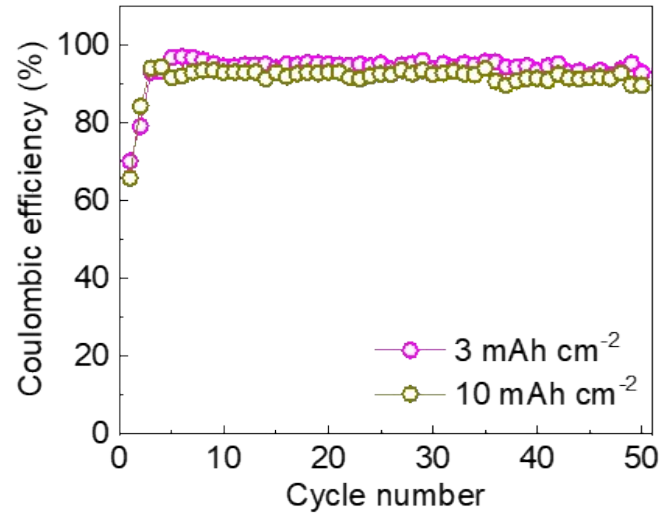Figure S13. HRTEM image of A/T-Nb$_2$O$_5$ after 10 cycles.

Figure S14. The coulombic efficiency of A/T-Nb_2O_5 electrode at 1.5 mA cm^{-2} (3 mAh cm^{-2}) and 5 mA cm^{-2} (10 mAh cm^{-2}).
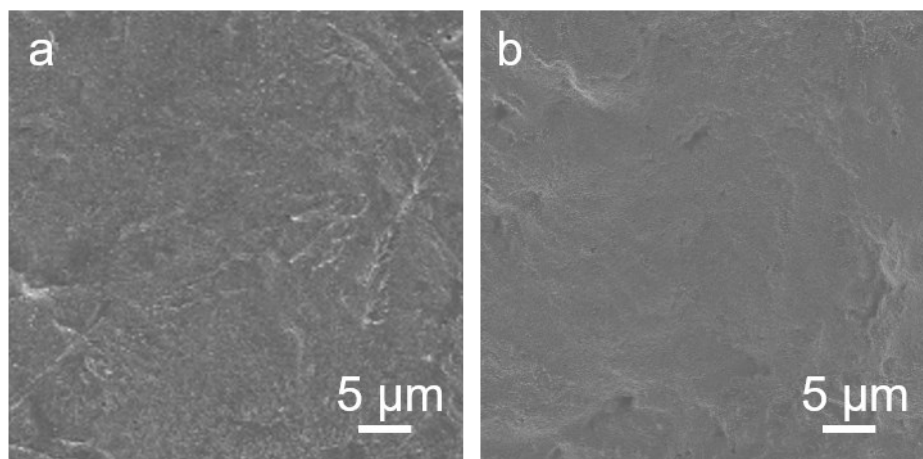
Figure S15. SEM image of (a) A-Nb$_2$O$_5$ and (b) T-Nb$_2$O$_5$ electrodes after 20 cycles at 1.5 mA cm^{-2} and 3 mAh cm^{-2}.
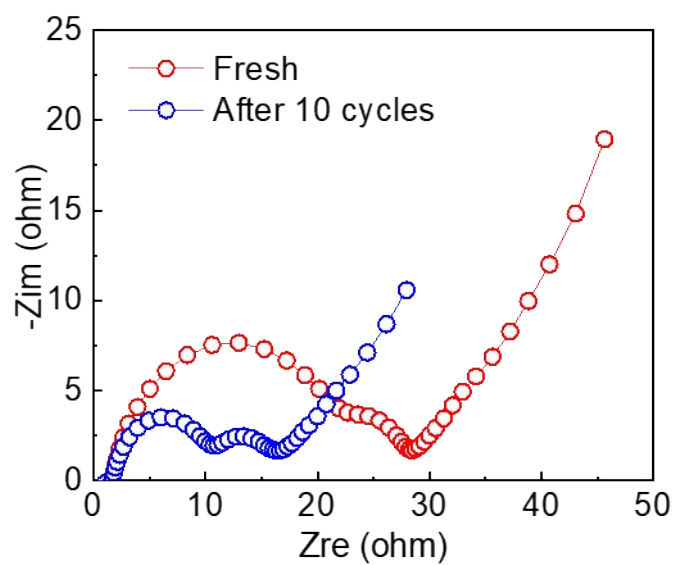
Figure S16. EIS spectra of the symmetric battery before and after cycling.

Table S1. The Li$^+$ diffusion coefficient at peak A for S-A-Nb$_2$O$_5$, S-A/T-Nb$_2$O$_5$ and S-T-Nb$_2$O$_5$ electrodes at different CV scanning rates.

	S-A-Nb$_2$O$_5$	S-A/T-Nb$_2$O$_5$	S-T-Nb$_2$O$_5$
0.1 mV s^{-1}	2.85×10^{-11} cm^2 s^{-1}	3.31×10^{-11} cm^2 s^{-1}	1.53×10^{-11} cm^2 s^{-1}
0.2 mV s^{-1}	3.18×10^{-11} cm^2 s^{-1}	4.07×10^{-11} cm^2 s^{-1}	1.92×10^{-11} cm^2 s^{-1}
0.3 mV s^{-1}	3.28×10^{-11} cm^2 s^{-1}	4.61×10^{-11} cm^2 s^{-1}	2.24×10^{-11} cm^2 s^{-1}
0.4 mV s^{-1}	3.26×10^{-11} cm^2 s^{-1}	4.73×10^{-11} cm^2 s^{-1}	2.42×10^{-11} cm^2 s^{-1}
0.5 mV s^{-1}	3.17×10^{-11} cm^2 s^{-1}	4.82×10^{-11} cm^2 s^{-1}	2.61×10^{-11} cm^2 s^{-1}